

Measurement of longitudinal spin transfer of the $\Lambda(\bar{\Lambda})$ hyperon in polarized p+p collisions at $\sqrt{s} = 200$ GeV at RHIC-STAR

Yi Yu for the STAR Collaboration

Institute of Frontier and Interdisciplinary Science & Key Laboratory of Particle Physics and Particle Irradiation (MOE), Shandong University, Qingdao, Shandong, 266237, China

E-mail: 201812156@mail.sdu.edu.cn

(Received January 15, 2022)

Since the first surprising results on the spin structure of the proton by the EMC experiment in the late 1980s, much progress has been made in understanding the origin of the proton spin. However, the sea quark contribution to the proton spin, for example, the helicity distributions of the strange quark (anti-quark), $s(\bar{s})$, is still not well constrained by experimental data. Since the $s(\bar{s})$ is expected to carry a substantial fraction of the spin of the $\Lambda(\bar{\Lambda})$ hyperon, measurements of the longitudinal spin transfer, D_{LL} , of the $\Lambda(\bar{\Lambda})$ hyperon can thus shed light on the helicity distribution of the $s(\bar{s})$ and the longitudinally polarized fragmentation functions. In these proceedings, we will present the status of the $\Lambda(\bar{\Lambda})$ D_{LL} analysis using data collected at RHIC-STAR in 2015, for the pseudo-rapidity $|\eta| < 1.2$ and transverse momenta up to 8.0 GeV/c. The D_{LL} as a function of the longitudinal momentum fraction of the $\Lambda(\bar{\Lambda})$ hyperon in the jet is also investigated. This data set is about twice as large as the 2009 data used for the previously published D_{LL} results.

KEYWORDS: proton helicity structure, RHIC-STAR, Λ hyperon, spin transfer

1. Introduction

Understanding the spin structure of the proton is one of the most challenging and fundamental questions in QCD. In 1988, the European Muon Collaboration published the puzzling result showing that the quark and anti-quark spin only contribute little to the spin of the proton [1]. This result then inspired global experimental and theoretical studies in the last 30 years. For the helicity structure of the proton, the contribution from valence quarks is well constrained [2]. However, the sea quark contributions, especially for the strange quark (anti-quark), $s(\bar{s})$, still have large uncertainties. Since the spin of the $\Lambda(\bar{\Lambda})$ hyperon is expected to be carried mostly by its valence $s(\bar{s})$, several theoretical studies [3–7] suggest that the D_{LL} can provide constraints on the helicity distribution of $s(\bar{s})$ and the polarized fragmentation functions of $\Lambda(\bar{\Lambda})$. In particular, Ref. [5] shows that measuring D_{LL} as a function of the jet momentum fraction (z) carried by the $\Lambda(\bar{\Lambda})$ hyperon can directly probe the polarized jet fragmentation functions of Λ and $\bar{\Lambda}$.

In polarized p+p collisions, the longitudinal spin transfer of Λ is defined as:

$$D_{LL} \equiv \frac{\sigma_{p^+p \rightarrow \Lambda^+X} - \sigma_{p^+p \rightarrow \Lambda^-X}}{\sigma_{p^+p \rightarrow \Lambda^+X} + \sigma_{p^+p \rightarrow \Lambda^-X}} = \frac{\Delta\sigma}{\sigma}, \quad (1)$$

where “+” or “-” denotes the helicity of the proton or $\Lambda(\bar{\Lambda})$. In the factorization framework, the polarized cross section $\Delta\sigma$ can be expressed as the convolution of the helicity distributions, partonic cross sections and polarized fragmentation functions.

The Relativistic Heavy Ion Collider (RHIC) is the world’s first and only polarized p+p collider which is capable of colliding the polarized proton beams at center of mass energies equal to 200

26 GeV and 510 GeV, making it an ideal facility for probing the spin structure of the proton. Previously,
 27 STAR has published the D_{LL} results [8] using the data taken in 2009 with an integrated luminosity
 28 of 19 pb^{-1} . In 2015, STAR recorded a larger data sample corresponding to an integrated luminosity
 29 of 52 pb^{-1} with an average beam polarization of about 54%. With this data set, we performed more
 30 precise measurements on the D_{LL} vs hyperon p_T and the first measurements on the D_{LL} vs hyperon
 31 momentum fraction (z) within jets.

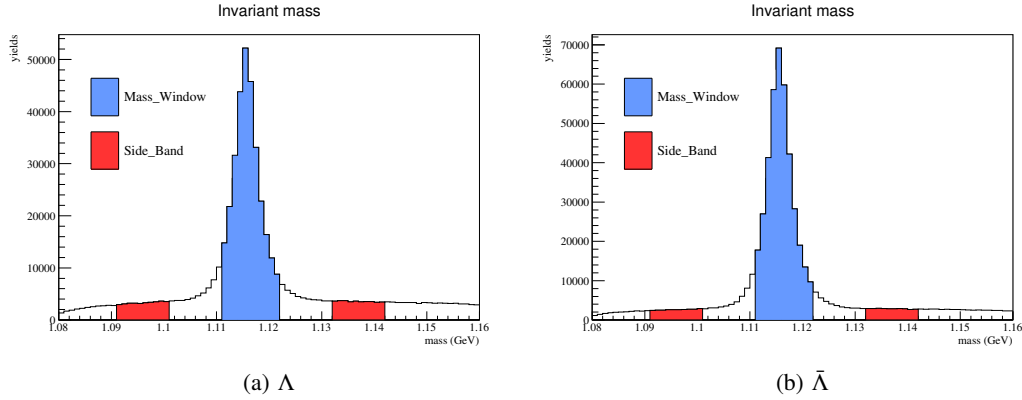


Fig. 1. Invariant mass distributions of Λ and $\bar{\Lambda}$ at $2 < p_T < 3 \text{ GeV}/c$. The hyperon yields under the mass peak (blue filled area) are used for the D_{LL}^{raw} calculation and the yields under the side-band region (red filled area) are used for estimating the background fraction under the hyperon mass peak.

32 2. Hyperon Reconstruction and D_{LL} Extraction

33 In this measurement, the $\Lambda(\bar{\Lambda})$ hyperons are reconstructed via the weak decay channel $\Lambda \rightarrow p + \pi^-$
 34 ($\bar{\Lambda} \rightarrow \bar{p} + \pi^+$). The proton and pion candidate tracks measured by the Time Projection Chamber
 35 (TPC) [9] are paired first, and then a set of topological selection criteria are applied to reduce the
 36 background fraction to the level about 10% under the hyperon mass peak, as presented in Fig. 1. To
 37 reconstruct the hyperon from the fragments of the outgoing parton, jets are first reconstructed using
 38 anti- k_T algorithm [10] with $R = 0.6$ using the tracks measured by the TPC and the energy deposits in
 39 the Barrel and Endcap Electromagnetic Calorimeter (BEMC/EEMC) [11, 12]. Then each hyperon is
 40 associated with a reconstructed jet by requiring $\Delta R = \sqrt{(\eta_{\Lambda(\bar{\Lambda})} - \eta_{jet})^2 + (\phi_{\Lambda(\bar{\Lambda})} - \phi_{jet})^2} < 0.6$.

41 The extraction of D_{LL} follows the same method as in [8, 13]. The polarization of the $\Lambda(\bar{\Lambda})$ can be
 42 obtained via the angular distribution of the $\Lambda(\bar{\Lambda})$ decay products in the hyperon rest frame:

$$\frac{dN}{d\cos\theta^*} = \frac{\sigma \mathcal{L} A}{2} (1 + \alpha_{\Lambda(\bar{\Lambda})} P_{\Lambda(\bar{\Lambda})} \cos\theta^*), \quad (2)$$

43 where the θ^* is the angle between the $\Lambda(\bar{\Lambda})$ momentum direction, i.e. longitudinal polarization direc-
 44 tion, and the momentum of its daughter $p(\bar{p})$ at the $\Lambda(\bar{\Lambda})$ rest frame, and A is the detector acceptance.
 45 The $\alpha_{\Lambda(\bar{\Lambda})} = 0.732(-0.732)$ [14] is the decay parameter and the $P_{\Lambda(\bar{\Lambda})}$ is the polarization of hyperons.
 46 To cancel the effect of the detector acceptance, the D_{LL} is measured in small $\cos\theta^*$ intervals using the
 47 following equation [13]:

$$D_{LL} = \frac{1}{\alpha_{\Lambda(\bar{\Lambda})} P_{beam} \langle \cos\theta^* \rangle} \frac{N^+ - \mathcal{R}N^-}{N^+ + \mathcal{R}N^-}. \quad (3)$$

48 Here, $N^+(N^-)$ denotes the hyperon yields with positive(negative) beam helicity, P_{beam} is the beam
 49 polarization and \mathcal{R} is the relative luminosity measured by the STAR Vertex Position Detector [15].

50 The raw spin transfers are extracted using the yields under the hyperon mass peak (blue area in
 51 Fig. 1) and are averaged over the whole $\cos\theta^*$ range. The residual background under the hyperon mass
 52 peak is mainly from random combinations of pion and proton candidates. This residual background
 53 is estimated using the side-band method (red area in Fig. 1). Its contribution to the D_{LL} is corrected
 54 using the following equation:

$$D_{LL} = \frac{D_{LL}^{raw} - rD_{LL}^{bkg}}{1 - r}, \quad (4)$$

55 where r is the residual background fraction under the hyperon mass peak.

56 3. D_{LL} Results

57 In this section, we present the new preliminary results of D_{LL} of Λ and $\bar{\Lambda}$. Section 3.1 presents
 58 the results of D_{LL} as a function of hyperon p_T , and Sec. 3.2 shows the first measurements on the D_{LL}
 59 versus hyperon z within jet.

60 3.1 D_{LL} vs hyperon p_T

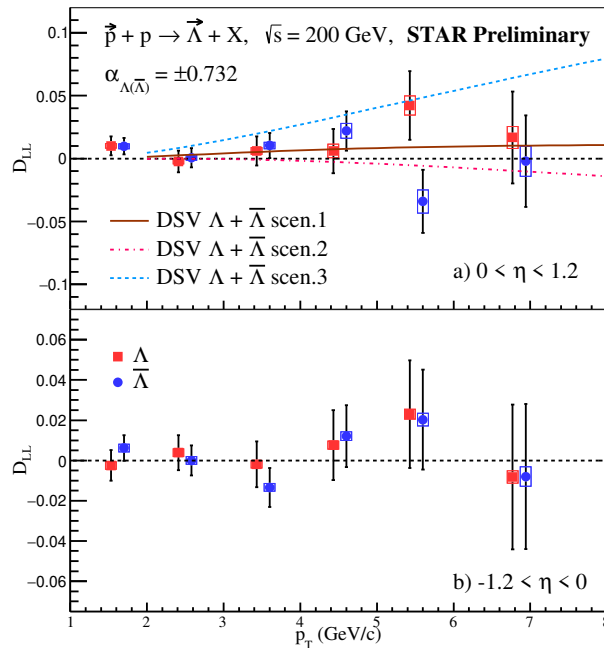


Fig. 2. Preliminary results of D_{LL} as a function of hyperon p_T for Λ and $\bar{\Lambda}$ in p+p collisions at $\sqrt{s} = 200$ GeV. The top panel is for positive hyperon η range and bottom one for negative η range with respect to the polarized proton beam. The theoretical curves are from Ref. [3].

61 Figure 2 shows the results of D_{LL} as a function of hyperon p_T in two different pseudo-rapidity
 62 ranges with respect to the momentum of the polarized proton. The results show consistency between

63 Λ and $\bar{\Lambda}$. The top panel shows the results for $0 < \eta < 1.2$. In this panel, the theoretical predictions [3]
 64 with different scenarios of the polarized fragmentation functions are compared with the measure-
 65 ments. The measurements are consistent with the model calculations within uncertainties.

66 3.2 D_{LL} vs z

67 In this measurement, z is defined as $z = \vec{p}_\Lambda \cdot \vec{p}_{jet} / |\vec{p}_{jet}|^2$, i.e. the longitudinal momentum fraction
 68 of the jet carried by the hyperon. The z value at detector level can be obtained with the reconstructed
 69 jet, i.e. detector jet. Since the theoretical calculations consider all produced particles in a jet, then the
 70 detector-level z needs to be corrected to the particle-level z . The correction is obtained with the Monte
 71 Carlo data based on the PYTHIA [16] and Geant [17] simulation.

72 The first results of D_{LL} versus z for Λ and $\bar{\Lambda}$ in p+p collisions at $\sqrt{s} = 200$ GeV are presented
 73 in Fig. 3. The jet p_T is required to be larger than 5 GeV/c. The top panel shows the results for the
 74 hyperon rapidity in the range of $0 < \eta < 1.2$ with respect to the momentum of the polarized beam and
 75 the bottom panel shows the results for $-1.2 < \eta < 0$. The results are compared with the theoretical
 76 predictions [5] for three scenarios of polarized fragmentation functions [18]. From Fig. 3, we can
 77 see that the results are consistent between Λ and $\bar{\Lambda}$. The data are also consistent with the model
 78 calculations. However, current measurement precision does not yet allow for a clear discrimination
 79 of different scenarios.

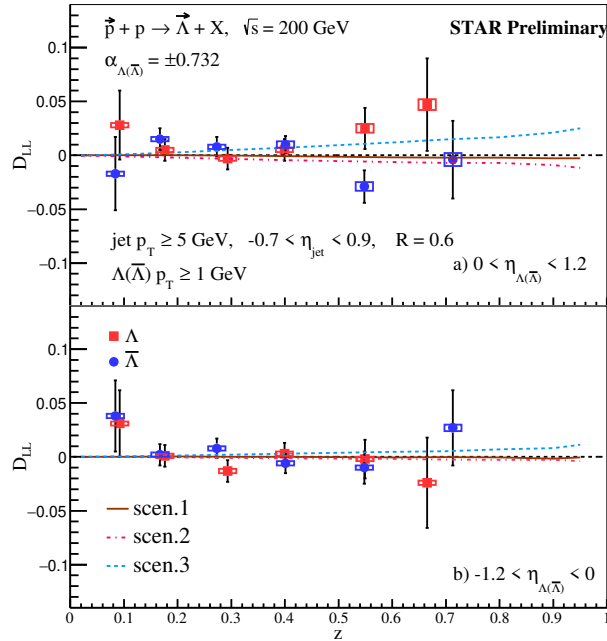


Fig. 3. Preliminary results of D_{LL} as a function of hyperon z for hyperon $p_T \geq 1.0$ GeV/c and jet $p_T \geq 5.0$ GeV/c. The top panel is for positive hyperon η range and the bottom one for negative η range with respect to the polarized proton beam. The theoretical curves are from Ref. [5] for three scenarios of polarized fragmentation functions.

80 **4. Summary**

81 In summary, new preliminary results on $\Lambda/\bar{\Lambda}$ longitudinal spin transfer D_{LL} vs p_T , and D_{LL} vs
82 hyperon z within a jet are presented for 200 GeV longitudinally polarized p+p collisions at STAR.
83 These measurements provide insights into the polarized fragmentation functions for the Λ and $\bar{\Lambda}$
84 hyperons and also the strange quark and anti-quark helicity distributions in the proton. The first
85 measurement of the D_{LL} vs z in polarized p+p collisions directly probes the polarized fragmentation
86 functions.

87 **Acknowledgements**

88 The author is supported partially by the National Natural Science Foundation of China under No.
89 12075140.

90 **References**

- 91 [1] J. Ashman et al. Phys Lett B **206**, 364 (1988).
92 [2] E.R. Nocera, R.D. Ball, S. Forte, G. Ridolfi, and J. Rojo, Nucl. Phys. B **887**, 276 (2014).
93 [3] D. de Florian, M. Stratmann, and W. Vogelsang, Phys. Rev. Lett. **81**, 530 (1998).
94 [4] Q. Xu, Z. Liang, and E. Sichterann, Phys. Rev. D **73**, 077503 (2006).
95 [5] Z.B. Kang, K. Lee, and F. Zhao, Phys Lett B **809**, 135756 (2020).
96 [6] X. Liu and B.-Q. Ma, Eur. Phys. J. C **79**, 409 (2019).
97 [7] B.-Q. Ma, I. Schmidt, J. Soffer, J.J. Yang, Nucl. Phys. A **703**, 346 (2002).
98 [8] J. Adam et al. [STAR Collaboration], Phys. Rev. D **98**, 112009 (2018).
99 [9] M. Anderson et al. [STAR Collaboration], Nucl. Instrum. Meth. A **499**, 659 (2003).
100 [10] M. Cacciari, G.P. Salam, and G. Soyez, J. High Energy Phys. **2008**, 063 (2008).
101 [11] M. Beddo et al. [STAR Collaboration], Nucl. Instrum. Meth. A **499**, 725 (2003).
102 [12] C.E. Allgower et al. [STAR Collaboration], Nucl. Instrum. Meth. A **499**, 740 (2003).
103 [13] B.I. Abelv et al. [STAR Collaboration], Phys. Rev. D **80**, 111102 (2009).
104 [14] P.A. Zyla et al. (Particle Data Group), Prog. Theor. Exp. Phys. **2020**, 083C01 (2020).
105 [15] W.J. Llope et al. [STAR Collaboration], Nucl. Instrum. Meth. A **759**, 23 (2014).
106 [16] T. Sjostrand, S. Mrenna, and P. Z. Skands, JHEP **05**, 026 (2006).
107 [17] R. Brun et al. CERN-W-5013 (1994).
108 [18] D. de Florian, M. Stratmann, and W. Vogelsang, Phys. Rev. D **57**, 5811 (1998).